Thermally Activated Coherent Vortex Motion in $YBa_2Cu_3O_{7-\delta}$ Thin Film Microbridges

M. J. M. E. de Nivelle, G. J. Gerritsma, and H. Rogalla
Department of Applied Physics, University of Twente, P.O. Box 217, 7500 AE Enschede, The Netherlands
(Received 4 August 1992; revised manuscript received 12 January 1993)

Microbridges with dimensions smaller than the London penetration depth λ have been prepared in epitaxial $YBaCu_2O_{7-\delta}$ thin films by means of electron beam lithography. Typical peaks and kinks are observed in their differential resistance versus current characteristics which can be attributed to coherent flux motion. A vortex activation energy proportional to the inverse current $1/I$ is obtained. Both the current and the temperature dependence of the activation energy are consistent with the collective flux creep model if the dimensionality of the elastic vortex lattice equals 2.

PACS numbers: 74.60.Ge, 74.60.Jg, 74.72.Bk, 74.76.Bz

It has been shown by Aslamazov and Larkin (AL) [1] in a theoretical paper that Abrikosov vortices will move coherently across the narrowest point of a superconducting microbridge if the width and length of this bridge are smaller than or comparable to the magnetic penetration depth λ. As a result, typical kinks will appear in the voltage-current (V-I) characteristics. This effect has been studied extensively regarding conventional superconductors [2, 3]. Only few observations have been reported so far for microbridges structured in films of high-T_c oxide superconductors with sufficiently small dimensions [4–6]. In the theory of AL thermally activated flux motion (TAFM) [7, 8] was not taken into account. However, it is well known by now that thermal activation of vortices plays an important role in high-T_c oxide superconductors ("giant" flux creep), except at very low temperatures [9–11]. In this Letter we report and discuss the resistive behavior and the nature of the vortex activation mechanism of very small microbridges structured in epitaxially grown (001) oriented $YBa_2Cu_3O_{7-\delta}$ (YBCO) thin films. The results are indicative of *thermally activated coherent* vortex motion.

We report the measurements on five typical microbridges with a length l of about 70 nm and widths w ranging from 950 down to about 175 nm which have been structured in a relatively smooth epitaxially grown YBCO film with a thickness d of about 85 nm. One of the bridges as observed with a scanning electron microscope (SEM) is shown in Fig. 1. This film was prepared by laser ablation on a (100) oriented yttria stabilized ZrO_2 substrate [12]. Before structuring a critical temperature $T_{c,0}$ of 87 K and a resistivity ratio $R(300\ \mathrm{K})/R(100\ \mathrm{K})=2.7$ was measured. For similar thin films structured into bridges with $w=10\ \mu$m and $l=100\ \mu$m we determined critical current densities between 1×10^{10} and 5×10^{10} A/m^2 at 77 K. A trilayer electron beam resist technique combined with argon plasma etching was used to pattern the film. To minimize the degradation of the superconducting properties of the YBCO film during the structuring process, all process temperatures were kept below 125 °C. The bridges showed critical temperatures between 83 and 87 K, with T_c decreasing systematically with decreasing width. Here T_c was determined from four-point measurements with a dc measuring current of 5 μA and a $R=0.2\ \Omega$ criterion which is about 1/50 of the observed normal state resistance just above the transition. The systematic decrease of T_c indicates that there is some degradation of the film quality starting at the etched boundaries of the bridge. Assuming a homogeneous current distribution across the microbridges and using a $dV/dI = 0.02\ \Omega$ criterion a critical current density at $T/T_c=0.85$ between 2×10^{10} and 3×10^{10} A/m^2 has been determined, which is close to the critical current density in high quality YBCO thin films. Thus we believe the transport properties are not dominated by weak

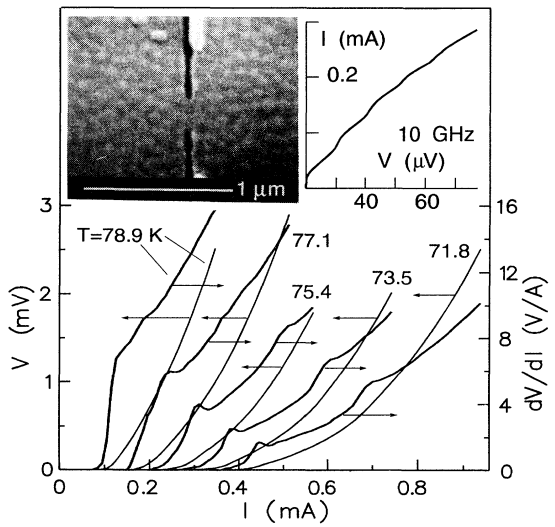

FIG. 1. V-I and dV/dI-I characteristics at different temperatures of a microbridge with $w \approx 225$ nm. The insets show a SEM picture of this microbridge, and a typical V-I characteristic with microwave induced Shapiro steps (T=56 K, f=10 GHz).

links in the microbridge region.

We have studied the differential resistance versus current (dV/dI-I) characteristics of the bridges for temperatures in the range 50 to 85 K. The differential resistance was measured by means of standard phase-sensitive detection and current modulation with a frequency of 120 Hz and amplitude of 5 μA. Some examples of the measured dV/dI-I characteristics together with the corresponding V-I characteristics obtained by numerical integration of the differential curves are shown in Fig. 1. Clearly visible are kinks or peaks in the dV/dI-I curves, which can be explained, at least qualitatively, within the model for small superconducting bridges proposed by AL. Thus, assuming that the bridge is symmetric and the vortex-antivortex pairs which are created at the edges of the bridge are moving towards the center of the bridge where they will annihilate with each other, the consecutive kinks along the dV/dI-I characteristics appear at voltage positions where the time average number of vortex-antivortex pairs present within the bridge equals an integer number. On increasing the current and passing such a kink, the energy barrier for the nucleation of vortices becomes higher, due to the additional repulsive interaction with one extra vortex or vortex pair, which is still present inside the bridge. The strongest peaks were observed for the bridges with estimated widths of 225 and 300 nm. Additional proof for the coherent motion of the vortices is obtained from V-I measurements with microwave irradiation. As can be seen in Fig. 1, Shapiro steps appear with the correct period $\Delta V = \Phi_0 f$, where Φ_0 is the flux quantum $h/2e$ and f is the frequency of the applied microwaves.

In Fig. 2, dV/dI-I curves for different temperatures of three typical bridges have been replotted with $\ln(I^2\,dV/dI)$ along the vertical axis and the inverse current $1/I$ along the horizontal axis. Plotted in this way, the data points below and above the kink show both approximately linear behavior. The current I_k at the position of the first kink and the position of the second kink will be discussed later. The linear behavior indicates that $dV/dI \propto (1/I^2)e^{-I_T/I}$, where I_T is a characteristic "activation" current. By integration with respect to the current we find $V \propto e^{-I_T/I}$, and

$$I^2\,dV/dI = I_T V. \tag{1}$$

This equation is in good agreement with Fig. 3(a), which shows the linear relation between $I^2\,dV/dI$ and V for currents $I > I_k$. By equating $e^{-I_T/I}$ to the standard $e^{-U/kT}$ probability function describing thermally activated processes, we obtain $U/kT = I_T/I$ or $U \propto I^{-1}$. This is clearly inconsistent with the usual TAFM potential $U \propto (1 - I/I_c)^\alpha$, with α=1 or 3/2 [8, 13]. However, agreement is possible with the vortex-glass model [14, 15] and the collective creep model [16], both yielding $U \propto I^{-\mu}$ (where μ is a positive exponent), if μ is near unity [17]. Recently, experimental evidence for the existence of the vortex-glass phase in YBCO thin films for current densities below 10^9 A/m^2 has been published [18]. An exponent $\mu \approx 0.19$ was determined for the vortex-glass phase, whereas for current densities above 10^{10} A/m^2 an exponent $\mu \approx 0.94$ was observed, which is close to our value $\mu \approx 1$. The latter current range coincides with the current densities in our measurements. In this range the dissipation is not dominated by the properties of the vortex glass but by the short-range interactions involving single vortex lines [18]. Envisioning the vortex lines as elastic strings moving along a two-dimensional random force plane it can be shown [19] that $U = \tilde{c}U_p^2/\Phi_0 J \propto I^{-1}$, where $\tilde{c}$ is the effective two-dimensional concentration of defects (e.g., oxygen vacancies) in the random force plane, U_p is the pinning energy of small pins, and J is the current density $\sim I/wd$. This is in fact an extension of the collective flux creep model [16]. Thus we obtain $U/kT = I_T/I$, with a characteristic current $I_T = \tilde{c}wdU_p^2/\Phi_0 kT$. Substitution of $U_p = B_c^2 V_c/\mu_0$, where B_c is the thermodynamical critical field and V_c is an elementary correlation volume, yields $I_T \propto (1 - t^2)^2/t$ ($t \equiv T/T_c$). Here we used $B_c \propto 1 - t^2$ and $V_c \approx \xi_{ab}^2 l_c$, where $\xi_{ab} = \xi_{ab,0}(1 - t^2)^{-1/2}$ is the coherence length along the a-b plane and l_c is the length

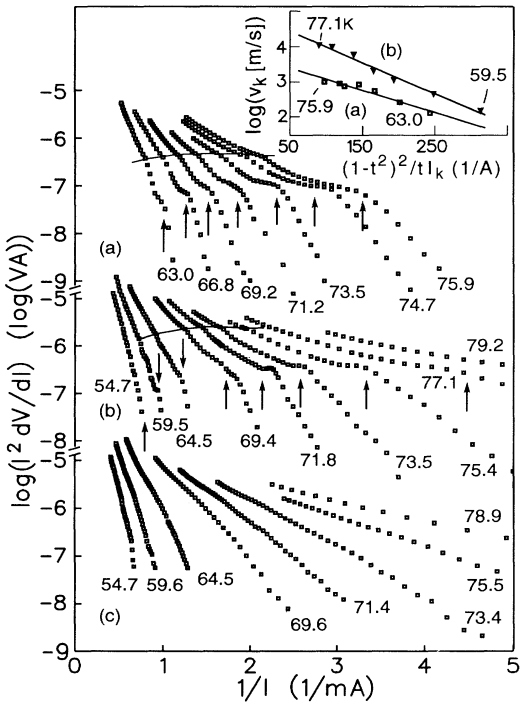

FIG. 2. The logarithm of $I^2\,dV/dI$ as a function of $1/I$ at different temperatures of three bridges. (a),(b) $w \approx 225$ nm and (c) $w \approx 175$ nm. The arrows point at the $1/I_k$ positions calculated for the temperatures of the corresponding curves. The solid curves mark the second kinks in the measurements. The inset shows the logarithm of the vortex velocity $v_k = V_k w/2\Phi_0$ vs $(1 - t^2)^2/tI_k$.

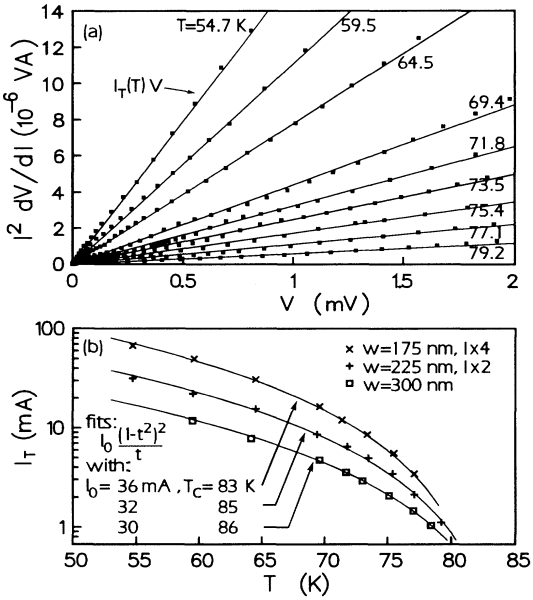

FIG. 3. (a) $I^2\,dV/dI$ vs V for different temperatures of the measurements shown in Fig. 2(b). (b) $I_T(T)$ determined from the linear slope in (a) and analogous plots not shown here for two other bridges. The solid curves are fits as indicated in the figure. The data points and fits of two bridges have been multiplied by 2 and 4, respectively, to avoid overlap.

of the correlation volume along the c direction which we approximate with the distance between the copper oxide planes.

Using Eq. (1), we have determined I_T for $I > I_k$ as a function of the temperature T from the slope of the linear $I^2\,dV/dI$-V plots. $I_T(T)$ can be accurately described with the temperature dependence derived above [Fig. 3(b)]. By substituting typical values I_T=5 mA, w=225 nm, d=70 nm, B_c=1 T, ξ_{ab}=2.5 nm, l_c=0.5 nm, T=70 K, and T_c=85 K, we obtain a realistic value for the two-dimensional concentration of defects, i.e., $\tilde{c} = 1/a^2$ with $a \approx$3 nm.

Because l is much smaller than the effective magnetic penetration depth $\lambda_\perp = \lambda \coth(d/2\lambda) \approx \lambda^2/d$ (i.e., $l \approx 70$ nm whereas $\lambda_\perp \approx 270$ nm for a typical value $\lambda \approx 150$ nm), vortices will move along the same path across the middle of the bridge in order to minimize their free energy [1]. Hence, making use of the Josephson relation $V = (\hbar/2e)d\phi/dt$ and taking into account that each vortex crossing the microbridge causes a phase shift $\Delta\phi = 2\pi$ between the two electrodes, the time average voltage over the bridge can be written as

$$V = \Phi_0 \nu e^{-U(I,T)/kT}, \tag{2}$$

where ν is an effective attempt frequency. Upon differentiating this equation and making use of Eq. (1), we obtain

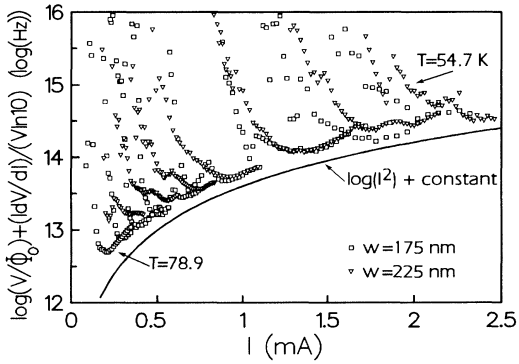

FIG. 4. The logarithm of the attempt frequency ν as a function of I, calculated for two bridges according to Eq. (3). For high enough currents all data follow an I^2 dependence as indicated by the solid curve.

$$\ln(\nu) = \ln\left(\frac{V}{\Phi_0}\right) + \frac{I\,dV/dI}{V\ln(10)}. \tag{3}$$

With this expression we have estimated the attempt frequency ν. In Fig. 4 the measurements of two bridges are replotted according to Eq. (3). At low currents the calculated ν decreases with increasing current, whereas at higher currents for all temperatures ν can be described with $\nu \approx 6 \times 10^{13}(I/[\mathrm{mA}])^2$ [s^{-1}]. Other observations of this remarkable current dependence or possible explanations are not known to us. Of course, if ν is strongly dependent upon I then Eq. (3) is not valid anymore. Therefore no direct conclusions can be attributed to the low current parts of all characteristics in Fig. 4. In the high current limit the plotted values are only weakly dependent upon I and Eq. (3) is a reasonable approximation.

Finally we compare the positions of the kinks with theory. From the theory of AL it follows that $I_k \sim (\Phi_0 d/4\mu_0\lambda^2)(w/\xi_{ab})^{1/2}$ [1, 3]. Substitution of $\lambda, \xi_{ab} \propto (1-t^2)^{-1/2}$ yields $I_k \sim I_{k0}(1-t^2)^{5/4}$, where $I_{k0} = (\Phi_0 d/4\mu_0\lambda_0^2)(w/\xi_{ab,0})^{1/2}$. With this relation we calculated the $1/I_k$ positions as indicated with the arrows in Fig. 2. Their positions agree rather well with the measurements. The fitted parameters I_{k0}=2.9 and 2.6 mA [Figs. 2(a) and 2(b), respectively] are close to I_{k0}=4.4 mA which is obtained by substituting realistic values d=70 nm, λ_0=250 nm, w=225 nm, and $\xi_{ab,0}$=2.5 nm. Furthermore, it is possible to calculate the average vortex velocity v_k at the position of the kink by substituting the voltage V_k at the first kink into the relation $v_k = wV_k/2\Phi_0$ [1]. Thus we have calculated v_k and plotted $\ln v_k$ vs $(1-t^2)^2/tI_k$ (Fig. 2, inset). An approximately linear relation is observed which is in accordance with the expressions $v_k = v_{k,0}e^{-I_T/I}$ and $I_T = I_0(1-t^2)^2/t$, where I_0=14.6 and 17.9 mA, and $v_{k,0} = 5.8 \times 10^3$ and 4.8×10^4 m/s, respectively. It can be verified that these

currents I_T are in approximate agreement with the slopes in Figs. 2(a) and 2(b) for $I \downarrow I_k$. By relating $v_{k,0}$ to an elementary attempt frequency ν_0 and a hopping distance a according to $v_{k,0} = \nu_0 a$, with $a \approx 3$ nm as estimated above, we obtain $\nu_0 = 2 \times 10^{12}$ and 2×10^{13} Hz. We note that the voltage at the second kink is approximately 4 to 8 times the voltage at the first kink (Fig. 1). This is not in accordance with the calculations of AL which give a factor of 2. One effect, not taken into account by AL, which could result in a higher ratio is that the velocity of the vortices increases when a new vortex nucleates at the edge of the bridge, as a result of their strong repulsive interaction [3]. Thus, as $v' > v$ where v' is the average vortex velocity at the second kink, the voltage at the second kink given by $V = \Phi_0 4v'/w$ [1] will be more than twice the voltage at the first kink [20].

In conclusion, microbridges with dimensions smaller than λ have been made in YBCO thin films which provide interesting information about the mechanism of the vortex motion. The observed $1/I$ dependence of the vortex activation energy is clearly different from the usual $(1-I/I_c)^\alpha$ dependence of the TAFM model. The current dependence can be explained by regarding the vortices as elastic strings moving in a two-dimensional random force field. The observed temperature dependence of the activation energy is also in agreement with this interpretation. An I^2 dependence has been determined for the involved attempt frequency.

We would like to thank R.P.J. IJsselsteijn for the film preparation and D. Terpstra for his support with the microwave measurements and some helpful discussions.

[1] L.G. Aslamazov and A.I. Larkin, Zh. Eksp. Teor. Fiz. **68**, 776 (1975) [Sov. Phys. JETP **41**, 381 (1975)].

[2] R.P. Huebener and D.E. Gallus, Phys. Lett. **44A**, 443 (1973); Phys. Rev. B **7**, 4089 (1973).

[3] H. Rogalla and C. Heiden, in *Superconducting Quantum Electronics*, edited by V. Kose (Springer-Verlag, Berlin, 1991).

[4] M.A.M. Gijs, D. Terpstra, and H. Rogalla, Solid State Commun. **71**, 995 (1989).

[5] H. Myoren, Y. Nishiyama, N. Miyamoto, Y. Osaka, and T. Hamasaki, Jpn. J. Appl. Phys. **28**, 2213 (1989).

[6] M.A.M. Gijs and R.J.E. Jansen, Appl. Phys. Lett. **56**, 1484 (1990).

[7] P.W. Anderson and Y.B. Kim, Rev. Mod. Phys. **36**, 39 (1964).

[8] M.R. Beasley, R. Labush, and W.W. Webb, Phys. Rev. **181**, 682 (1969).

[9] Y. Yeshurun and A.P. Malozemoff, Phys. Rev. Lett. **60**, 2202 (1988).

[10] M. Tinkham, Phys. Rev. Lett. **61**, 1658 (1988).

[11] R. Griessen, J.G. Lensink, and H.G. Schnack, Physica (Amsterdam) **185-189C**, 337 (1991).

[12] D.H.A. Blank, D.J. Adelerhof, J. Flokstra, and H. Rogalla, Physica (Amsterdam) **167C**, 423 (1990).

[13] L. Fruchter, A.P. Malozemoff, I.A. Campbell, J. Sanchez, M. Konczykowski, R. Griessen, and F. Holtzberg, Phys. Rev. B **43**, 8709 (1991).

[14] D.S. Fisher, M.P.A. Fisher, and D.A. Huse, Phys. Rev. B **43**, 130 (1991).

[15] R.H. Koch, V. Foglietti, W.J. Gallagher, G. Koren, A. Gupta, and M.P.A. Fisher, Phys. Rev. Lett. **63**, 1511 (1989).

[16] M.V. Feigel'man, V.B. Geshkenbein, A.I. Larkin, and V.M. Vinokur, Phys. Rev. Lett. **63**, 2303 (1989).

[17] It has been shown [14] that the thermal nucleation of vortex loops in the Meissner phase directly yields $U \propto 1/I$. However, the energy scale involved is too high to apply to our measurements.

[18] C. Dekker, W. Eidelloth, and R.H. Koch, Phys. Rev. Lett. **68**, 3347 (1992).

[19] L.B. Ioffe and V.M. Vinokur, J. Phys. C **20**, 6149 (1987).

[20] Recent computer simulations of the vortex motion, making use of the full expression for the forces in a microbridge [3], showed us ratios between 2.7 and 4.6 for reasonable values of ξ, w, d, and λ. Another explanation of the second kink might be that the vortices start moving along two parallel paths.

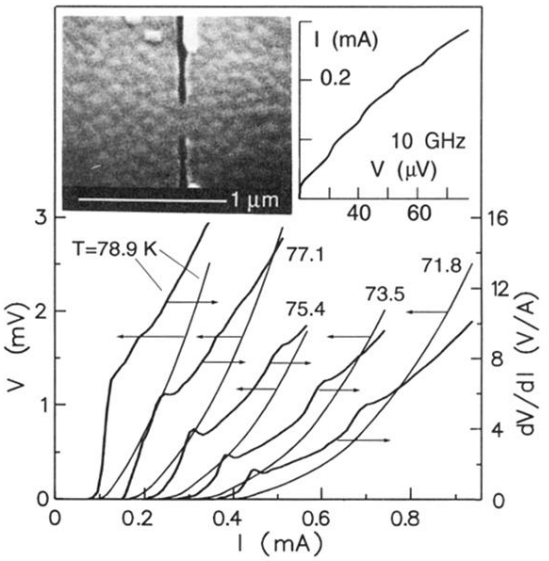

FIG. 1. V-I and dV/dI-I characteristics at different temperatures of a microbridge with $w \approx 225$ nm. The insets show a SEM picture of this microbridge, and a typical V-I characteristic with microwave induced Shapiro steps (T=56 K, f=10 GHz).